PECULIARITIES OF RAMAN SPECTRA SHAPE IN THE DISORDERED FERROELECTRICS

M.D. Glinchuk, I.V. Kondakova

February 1, 2008

Institute for Material Sciences, National Academy of Sciences of Ukraine, Krzhizhanovskogo str. 3, 252180 Kiev, UKRAINE

Abstract

Theory of the first order Raman scattering (FOR) line shape allowing for nonlinear and correlation effects contribution to inhomogeneous broadening as well as dynamic mechanisms of homogeneous broadening is developed. It is shown that in general case FOR line contains two maxima, shape of low frequency one being defined by homogeneous broadening. Our theory explains the peculiarity of observed FOR scattering of TO_2 hard phonon in KTL and KTN at different temperatures and concentrations of Li and Nb ions.

1 Introduction

Investigation of Raman spectra of the first order (FOR) in disordered ferroelectrics was shown to be sensitive method for studying of the critical slowing down of optic phonons nearby ferroelectric transition and dynamics of local fluctuation (see e.g. [1, 2] and ref. therein). Several attempts were made to explain FOR spectral anomalies such as strong increase of peak intensity in the vicinity of T_c and peculiar shape of the line [3] . However, up to now there is no general approach to the description of Raman spectra in the disordered ferroelectrics nearby T_c. These results are in the discrepancy in the values of the materials physical characteristics obtained from experimental data (see e.g. [1] -[4]). The most promising way for development of general approach seems to be the model allowing for inhomogeneous broadening of FOR lines induced by static disorder and homogeneous broadening due to dynamic effects. The existence of both these contributions to Raman spectra was shown early in $KTa_{1-x}Nb_xO_3$ (KTN) and $K_{1-x}Li_xTaO_3$ (KLT) [1, 2, 3].

Theory of inhomogeneously broadened lines in radio-, optic- and other spectroscopy methods was developed in many details early for conventional dielectric and magnetic systems [5, 6]. In these materials inhomogeneous broadening used to be temperature independent,

so that only homogeneous broadening may be the source of temperature dependence of the spectra line shape and width. In the disordered ferroelectrics due to nonlinear and spatial correlation effects which is known to be especially strong in the vicinity of T_c inhomogeneous broadening was recently shown to be temperature dependent [7] .

In the present work a theory of FOR allowing for both linear and nonlinear contributions to inhomogeneous broadening as well as to homogeneous mechanisms of line broadening is developed. The theory explains the main peculiarities of observed FOR spectra in KTL with 1% and 4% of Li [3] and in KTN with 15.7% of Nb ions [2] when the systems approach the phase transition from above. Since in vicinity of the phase transition the nonlinear effects are known to be large enough our theory is more general than that in [2, 3] , where nonlinear and spatial correlation effects were not taken into account. The proposed theoretical approach allows to describe of the Raman spectra (in distingvish [2, 3]) without calculation of the correlation function of the quasi-static polarization fluctuations but only suggesting about its spectral density form. Because of generality of proposed theory it can be applied to many ferroelectrics in vicinity of transition temperature.

2 Theory of first order Raman spectra shape

2.1 Incipient ferroelectric $KTaO_3$ doped by Li or Nb ions can have ferroelectric phase transition, mixed ferroglass phase and dipole glass state in dependence on temperature and the impurities concentrations [8, 9]. These materials can be regarded as the model systems of the disordered ferroelectrics. Their peculiar properties are connected with off-center positions of Li and Nb ions substituted for K^+ and Ta^{5+} ions respectively. Some anomalies of Raman spectra can be explained also by these ions off-centrality. In particular quasistatic polarization fluctuations induced by off-center ions can lead to the reduction of $KTaO_3$ cubic symmetry and to the appearance of first order Raman scattering (FOR) even above the transition temperature T_c [1, 3]. The most detail description of the appeareance of the single phonon Raman lines above T_c can be found in [10] where it was shown how the slow finite-range precursor order, dominant near the phase transition, is responsible for the persistence of quasi-first-order hard-mode features above T_c.

As known, Raman scattering in perovskite ferroelectrics is caused by the changes in the oxygen electrtonic polarizability $\delta\alpha(r,t)$ induced by optic vibration modes of the lattice. This changes can be written in the form

$$\delta\alpha(r,t) = \mathbf{P}(\mathbf{r},\mathbf{t}) \cdot \hat{\mathbf{\Lambda}} \cdot \mathbf{P}(\mathbf{r},\mathbf{t}) \tag{1}$$

where $P(r,t)$ represents the space- and time-dependent polarization fluctuation and $\hat{\Lambda}$ is a fourth-rank tensor. Equation (1) usually describes second-order Raman scattering. However, if we write the fluctuation polarization as a sum over the components due to the polar hard modes P^h and slow relaxing component P^μ we can explain the appearance of single-phonon Raman scattering above T_c considering the cross terms $P^\mu P^h$ in the Eq.(1) The scattering intensity is given by the spatial and temperature Fourier components of the polarizability

correlation function

$$I(\omega) \sim < \delta\alpha(r,t)\delta\alpha(0,0) >_{q=0,\omega}$$
$$\sim \sum_{q'} \int d\omega' < P^{\mu}(r,t)P^{\mu}(0,0) >_{q',\omega'} < P^{h}(r,t)P^{h}(0,0) >_{-q',\omega-\omega'} , \qquad (2)$$

Because the first correlation function has a sharp maximum near $\omega' = 0$ and second one near Ω_q, $I(\omega)$ is sharply peaked at $\omega = \Omega_q$, i.e., near the hard single-phonon frequency.

It is seen that (2) can be represented as the convolution of the functions represented inhomogeneous and homogeneous mechanisms of broadening connected respectively with the first and the second correlators and so it can be written in the form

$$I(\omega) = I_0 \int_{-\infty}^{\infty} J(\omega,\omega')\, f(\omega') d\omega' \, . \qquad (3)$$

The detailed form of homogeneuos $J(\omega,\omega')$ and inhomogeneous contribution $f(\omega')$ can be obtained by the following way. Thermal lattice vibrations usually lead to homogeneous broadening with simple Lorentzian shape, i.e.

$$< P^{h}(r,t)P^{h}(0,0) >_{-q',\omega-\omega'} \sim -\frac{1}{\Omega_{q'}} \frac{\Gamma}{\Gamma^2 + (\omega - \omega' - \Omega_{q'})^2} , \qquad (4)$$

which should be valid for the difference of frequencies $(\omega - \omega')$ close to hard phonon frequency $\Omega_{q'}$. On the other hand the correlation function of quasistatic polarization reads

$$< P^{\mu}(r,t)P^{\mu}(0,0) >_{q',\omega'} = < P^{\mu}(r)P^{\mu}(0) >_{q'} \ \pi\delta(\omega') \, . \qquad (5)$$

Substituting (long-wave approximation) $\sum_{q'} \to \frac{V}{(2\pi)^3} \int d^3q'$ and performing some transformation one obtaine that

$$f(\omega') = \int dq'\, q'^2 < P^{\mu}(r)P^{\mu}(0) >_{q'} \delta(\omega' - \Omega_{q'}) \frac{1}{\Omega_{q'}} , \qquad (6)$$

$$J(\omega,\omega') = \frac{\Gamma}{\Gamma^2 + (\omega - \omega'^2)}, \qquad I_0 = \frac{V}{2\pi} \, . \qquad (7)$$

Equations (6) and (7) determine respectively the contribution of inhomogeneous and homogeneous broadening into Raman line shape (see Eq. (3)). However it is seen from Eq. (6), that for $f(\omega)$ calculation one has to calculate firstly the correlation function of polarization. Its calculation utilized some special models and supposition [1, 3] . To our mind more general approach for $f(\omega)$ calculation can be statistical theory of specrtal line shape [5]. This theory was sucsessfully applied for description of optic, radiospectrroscopy, γ-resonance etc. line shapes [6, 11].

2.2 The shape of $f(\omega)$ was calculated in the statistical theory framework for the cases when the frequency shift of spectral line is linear [5, 6] and nonlinear [7, 11] function of random fields. The latter case seems to be especially important for disordered ferroelectrics at $T = T_c \pm \Delta T$, $\Delta T \simeq (10 \div 20)K$, where nonlinear and correlation effects is known to be

large enough. As a matter of fact the distribution function allowing for these effects can be expressed via linear one in the framework of the general theory of probability which makes it possible to write down the distribution of one random quantity via that of another if the relation between these quantities is known [12]. For example in the simplest case when the random quantity x is a single-valued monotonous function of another random quantity h then the relation between their distribution functions $g(h)$ and $f(x)$ can be written as [12]

$$g(h) = f(x(h)) \left| \frac{dx(h)}{dh} \right| . \tag{8}$$

In general case when several different x values correspond to the same $h(x)$ value the space of x should be devided into the regions where the function $h(x)$ is monotonous. For the entire x-domain distribution function $g(h)$ can be represented as a sum of terms like Eq.(8) [7, 11, 12]. Since the distribution function in the case of linear contribution of the random field $f_1(\omega)$ can be analytically calculated in statistical theory approach [5, 6] we have to express via it the distribution function allowing for nonlinear random field contribution. Let us suppose that the shift $\Delta\omega = \omega - \omega_0 \equiv \omega$ of the spectral line maximum position $\omega 0$ due to random field contribution can be written as a power law (up to some m^{th} power) of the random field ω'

$$\omega = \omega' - \alpha_2 \omega'^2 - \ldots - \alpha_m \omega'^m . \tag{9}$$

Equation (9) makes it possible to express the distribution function of ω via that of ω' in the form [7, 11, 12]

$$f_m(\omega) = \sum_{k=1}^{m} f_1 \left(\omega' = \omega_k\right) \left| \frac{d\phi(\omega, \omega')}{d\omega'} \right|_{\omega' = \omega_k} , \tag{10}$$

$$\phi(\omega, \omega') = \omega - \omega' - \alpha_2 \omega'^2 - \ldots - \alpha_m \omega'^m . \tag{11}$$

where ω_k are the real roots of the algebraic equation

$$\phi(\omega, \omega_k) = 0 . \tag{12}$$

It is seen, that m^{th} order distribution function $f_m(\omega)$ is expressed via that calculated in linear approximation when all nonlinear coefficients equal zero, i.e. $\alpha_2 = \alpha_3 = \ldots = \alpha_m = 0$. Shape of $f_1(\omega)$ calculated in the statistical theory approach was shown to be Gaussian, Lorentzian or Holtzmarkian in dependence on types of random field sources with parameters determined by the sources concentrations and characteristics [9, 6].

In the simplest case, when the main contribution is connected with the first nonlinear term in Eqs. (9), (11) ($\alpha_2 \neq 0, \alpha_3 = \ldots = \alpha_m = 0$) Eqs.(10), (11) and (12) lead to the following form of the normalized second order distribution function

$$f_2(\omega) = \frac{\Theta\left(\omega + \frac{1}{4\alpha_2}\right)}{\sqrt{1 + 4\alpha_2\omega}} \left[f_1\left(\frac{\sqrt{1 + 4\alpha_2\omega} - 1}{2\alpha_2} \right) + f_1\left(-\frac{\sqrt{1 + 4\alpha_2\omega} + 1}{2\alpha_2} \right) \right] , \tag{13}$$

where Θ is the teta-function, so that $f_2 \neq 0$ only in region $\omega_c \leq \omega \leq \infty$ ($\alpha_2 > 0$) or $-\infty \leq \omega \leq \omega_c$ ($\alpha_2 < 0$),

$$\omega_c = -(1/4\alpha_2) \tag{14}$$

is a critical frequency at which a divergency of $f_2(\omega)$ appears. Therefore $f_2(\omega)$ is strongly asymmetrical, and its form at $\omega \gg \omega_c$ (the wing of $f_2(\omega)$) is the following

$$f_2(\omega) \to 1/\sqrt{1+4\alpha_2\omega}\,. \tag{15}$$

Let us consider the homogeneous contribution in the Lorentzian form (see Eq.(7)). In this case the integration in Eq.(3) is equivalent to substitution $\omega \pm \frac{i}{\tau}$ for ω in the Eq.(13) ($1/\tau \equiv \Gamma$ is half width on the half height). If there are several mechanisms of homogeneous broadening with Lorentzian forms $1/\tau = \sum_i 1/\tau_i$, where i numerates the mechanisms.

The aforementioned procedure (or integration in Eq.(3)) with respect to Eq.(13) in supposition that $f_1(\omega)$ has Gaussian form, i.e.

$$f_1(\omega) = \frac{1}{\sqrt{2\pi}} e^{-\frac{\omega^2}{2\Delta^2}}\,, \tag{16}$$

leads to the following shape of spectral line in the considered case

$$I_2(\omega) = \frac{\frac{1}{2} + \frac{1}{\pi}\arctan\tau(\omega-\omega_c)}{\Delta\sqrt{2\pi\varphi(\omega)}} \left\{ \exp\left[\frac{S_1(\omega) - 2(1+2\alpha_2\omega)}{8\alpha_2^2\Delta^2}\right] \cos\frac{4\alpha_2/\tau - S_2(\omega)}{8\alpha_2^2\Delta^2} \right.$$
$$\left. + \exp\left[\frac{-S_1(\omega) - 2(1+2\alpha_2\omega)}{8\alpha_2^2\Delta^2}\right] \cos\frac{4\alpha_2/\tau + S_2(\omega)}{8\alpha_2^2\Delta^2} \right\}, \tag{17}$$

where

$$\varphi(\omega) = \sqrt{(1+4\alpha_2\omega)^2 + (4\alpha_2/\tau)^2}\,,$$
$$S_{1,2}(\omega) = \sqrt{2}\sqrt{\varphi(\omega) \pm (1+4\alpha_2\omega)}\,.$$

The results of numerical calculations for several values of dimensionless parameters $\alpha_2\Delta$ and $1/(\tau\Delta)$ are depicted in figs. 1,2. It is seen that homogeneous contribution transforms $f_2(\omega)$ divergence at $\omega = \omega_c$ into sharp maximum, so that the spectral line has two maxima (see fig. 1) instead of one in the linear case origin of high frequency one being connected with Gaussian form. The distance between two maxima approximately equals ω_c (see fig. 1). At large enough nonlinear contribution only sharp maximum at $\omega = \omega_c$ conserves, its width increases with $1/\tau$ increasing (see fig. 2). The left hand side half-width of low-frequency peak completely defined by homogeneous broadening mechanisms, meanwhile right hand side part of the line at $\omega > \omega_c$ defines mainly by inhomogeneous mechanism contribution.

3 Raman spectra in KTL and KTN

3.1 The developed theory was applied to recently observed TO_2 FOR in KTL with 1% and 4% of Li and in KTN with 15.7% of Nb [3, 2].

Let us begin with the consideration of Raman spectra in KTL. Measurements were carried out at $T = 10$ K ($x_{Li} = 0.01$) and $T = 55$ K ($x_{Li} = 0.04$) [3]. In both samples

the observed line was strongly asymmetric with maximum at $\omega \simeq 198$ cm^{-1}. These lines were fitted good enough by Eqs. (12) - (14) with the following dimensionless parameters $\alpha_2\Delta = 0.38$, $(\tau\Delta)^{-1} = 0.06$ (fig. 3) and $\alpha_2\Delta = 0.55$, $(\tau\Delta)^{-1} = 0.15$ (fig. 4) for the considered Li concentrations respectively.

The position of the lines maxima $\omega_m - \omega_0 = \omega_c$ is defined by the parameter of nonlinearity in accordance with Eq. (14). We obtained $\alpha_2 \simeq 0.1$ cm by the fitting of the high frequency line tails with the Eq.(15). This value gives $\omega_m = \omega_c + \omega_0 \simeq 197.6$ cm^{-1} with the reference point $\omega_0 = 199$ cm^{-1}. Note that Eq.(15) describes also observed frequency dependence of the lines tails for the same α_2 value. This made it possible to obtaine yhe magnitude of the Gaussian width Δ with the help of aforemationed $\alpha_2\Delta$ values: $\Delta = 3.8$ cm^{-1} ($x_{Li} = 0.01$) and $\Delta = 5.5$ cm^{-1} ($x_{Li} = 0.04$).

In accordance with our theory the line form at $\omega < \omega_c$ defines completely by homogeneous mechanism contribution represented by Eq.(4). It is seen that low-frequency half-width $1/\tau$ is connected with hard phonon life time Γ^{-1}. Keeping in mind the obtained values of $(\tau\Delta)^{-1} \equiv \Gamma/\Delta$ and Δ one find Γ ($T = 10$ K) $\simeq 0.25$ cm^{-1}, Γ ($T = 55$ K) $\simeq 0.8$ cm^{-1}. These date are in resonable agreement with ordinary values of hard phonon life times and with observed low-frequency half-width (see figs 3, 4).

3.2 Now let us proceed to consideration of Raman spectra in KTN with 15.7% Nb which has the transition from cubic to tetragonal phase at $T_c = 138.6$ K. The measurements were carried out at several temperatures in vicinity of T_c: $T = 160$, 150, 146 and 142 K [2]. At all the temperatures the lines with two maxima were observed, the first being nearby $\omega_1 \simeq 200$ cm^{-1} and the second at $\omega_2 \simeq 220$ cm^{-1}. The intensity of low frequency maximum essentially increased with T lowering, meanwhile the intensity of high frequency one became very small at $T = 142$ K. Since nonlinear parameter α_2 increases with temperature approaching to T_c [11], nonlinear effects has to be the largest at $T = 142$ K. Qualitatively transformation of spectra from two-peak line to one-sharp peak line at nonlinear parameter increasing is in agreement with theoretical overcasting (see figs.1, 2) It is seen also that increasing of low frequency maximum intensity with T lowering can be the result of $1/\tau$ decreasing.

To be sure that nonlinear effects are really responsible for observed Raman spectra transformation we checked if the Eqs.(13-15) fitted experimental spectra. It was shown that Eq.(15) fitted the wing ($\omega \geq 230$ cm^{-1}) of Raman line at $T = 142$ K for $\alpha_2 \simeq 0.015$ cm, which lead to $\omega_c \simeq 20$ cm^{-1} (see Eq. (14)). This value fits pretty good the distance between two peaks of observed Raman spectra (see fig. 5), which speaks in favour of nonlinear effects contribution. In fig. 5a we depicted line shape calculated with the help of Eq. (17) for $\alpha_2 = 0.012$ cm and $\Delta \simeq 17$ cm^{-1}. The later quantity was taken from measured high frequency maximum width. Note, that obtained Δ value made it possible to fit dimensionless ω/Δ scale with ω scale in fig. 5 and later in fig. 6.

The values of homogeneous broadening parameter $1/\tau$ at different T were calculated in supposition that it defines mainly by reorientational frequency of elastic dipole connected with Nb. This frequency temperature dependence was measured early [13] and it was de-

scribed by Arrenius law

$$\frac{1}{\tau} = \frac{1}{\tau_0} \exp(-U/T) \tag{18}$$

with U=200 K and $1/\tau_0 = 7 \times 10^9$ Hz. At $T = 150$ K Eq.(13) leads to the value $(\tau\Delta)^{-1} \simeq 0.004$, which was used in calculation of the line, depicted in fig. 5a. It is seen from fig. 5 that the calculation and observed spectra look like one another.More detailed comparison of the theory and experiment was carried out for Raman line observed at $T = 142$ K (see fig. 6). Theoretical curve was drawn for aforementioned parameter $\alpha_2 = 0.015$ cm, obtained from line wing behaviour and $1/\tau$ was calculated with the help of Eq.(18). It is seen that theory fits pretty good observed Raman spectra. This gave evidence that measured Raman line asymmetry and rapid change in line shape when approaching the transition from above is really connected with nonlinear effects in KTN with 15.7% Nb. Theory overcasts strong increasing of low frequency peak at the region 142 K $> T > T_c$ because of α_2 increasing and $1/\tau$ decreasing in supposition that there is no another even small temperature independent contribution to $1/\tau$.

Comparing the obtained data for KTL and KTN one can see that because the reorientation rate of Nb dipoles is much larger than that of Li, the homogeneous broadening of Raman line in KTL is defined by hard phonon dynamic whereas in KTN - by Nb elastic moment reorintation. Note that in [2, 3] the reorientation of Nb electric dipole moment were supposed to be the origin of the homogeneous broadening. However the parameters of the electric dipoles orientations obtained from fitting of the theory with the experiment were strongly different from those obtained early in independent measurements [14].

4 Discussion

The proposed theoretical description of Raman spectra shapes was perfomed without calculation of correlation function of quasy-static fluctuation of polarization. The comparison with the caculations of Raman spectra based on calculation of this correlation function shows that the parameter $\alpha_2\Delta$ corresponds to $v_h^2/\omega_0^2 r_c^2$ where v_h, Ω_0 and r_c are, respectively, a sound velosity, hard mode frequency at $q = 0$ and the correlation length of the polarisation in the pure lattice. These physical quantities define temperature and concentrational dependence of obtained values of $\alpha_2\Delta$. The value of parameter R_c/r_c (R_c is correlation radius of the lattice with impurities) defines the ratio of inhomogeneous and homogeneous contributions and at $T \to T_c$ ($R_c \to \infty$) the line becomes completely inhomogeneous [3] . In our approach the parameter of nonlinearity strongly increases with $T \to T_c$ and becomes much greater than homogeneous contribution which tends to decrease the magnitude of line maximum. Therefore qualititavely our results are in agreement with those obtained in [3] .

However comparing the frequency dependence of $J(\omega)$ at large ω one can see that it was described as $(\omega - \Omega_0)^{-3/2}$ [3] whereas in our theory as $(1 + 4\alpha_2\omega)^{-1/2}$. More accurate measurements of line intensity decay could be desirable for both theory comparison. Moreover, our theory gives the line shape with two maxima for intermidiate values of $\alpha_2\Delta$, which looks like that observed in KTN (see fig. 5). Thus the observed line shape with two maxima natu-

rally appeares in our theory whereas the second maximum was not obtained in the previous theoretical description [2]. Its origin was supposed to be some forbidden transition related to the mixture of acoustic and optic modes.

Therefore peculiarities of Raman spectra shape were explained by proposed theory. In particular it was shown that nonlinear effects leads to strong assymetry of the lines and to appearing of the low frequency sharp maximum, its left hand side is defined by dynamic properties of the system. The division between dynamic and static characteristics contribution into Raman spectra shape makes possible to investigate separately the both aforementioned characteristics by Raman spectroscopy method.

References

[1] H.Uwe,K.B.Lyons, H.L.Carter, P.A.Fleury, Phys.Rev.**B33**, 6436 (1986);

[2] B.E.Vugmeister, P.Di Antonio, J.Toulouse, Phys.Rev.Lett.,**75**, 1646 (1995);

[3] P.Di Antonio, B.E.Vugmeister, J.Toulouse, L.A.Boatner Phys.Rev.,**B47**, 5629 (1993);

[4] I.P.Sokoloff, L.L.Chase, L.A.Boatner, Phys. Rev.**B41**, 2398 (1990);

[5] A.U.Stoneham, Rev.Mod.Phys. **41**, 82 (1969);

[6] M.D.Glinchuk, V.G.Grachev, M.F.Deigen, A.B.Roitcin, L.A.Suslin, Elektricheskie effekty v radiospektroskopii, Nauka, Moscow (1981);

[7] M.D.Glinchuk, I.V.Kondakova, Fizika Tverdogo Tela, **40**, 340 (1998);

[8] M.D.Glinchuk, V.A.Stephanovich, J. Phys.: Condens. Matter, **6**, 6317 (1994);

[9] M.D.Glinchuk, V.A.Stephanovich, Ferroelectrics, **169**, 281 (1995)

[10] A.D.Bruce, W.Taylor and A.F.Murray, J. Phys.C: Solid St. Phys. **13**, 483 (1980).

[11] M.D.Glinchuk, I.V.Kondakova, Mol. Phys. Rep., **18/19**, 27 (1997);

[12] D.J.Hudson, Statistics, Geneva (1964);

[13] T.V.Antimirova, M.D.Glinchuk, A.P.Pechenyi, I.M.Smolyaninov, Fizika Tverdogo Tela, **32**, 208 (1990);

[14] U.T.Hochli, K.Knorr, A.Loidl, Adv.Phys., **39**, 405 (1990).

Figure captions

Figure 1. Line shape calculated on the base of Eq.(9) for $\alpha_2\Delta$ =0.22 and $(\tau\Delta)^{-1}$= 0.3 (curve 1), 0.01 (curve 2); doted line is Gaussian form.

Figure 2. Line shape calculated on the base of Eq.(9) for $\alpha_2\Delta$ =0.4 and $(\tau\Delta)^{-1}$ = 0.1 (curve 1), 0.05 (curve 2), 0.01 (curve 3); doted line is Gaussian form.

Figure 3. FOR scattering line shape, solid line - theory at $\alpha_2\Delta$ =0.38 and $(\tau\Delta)^{-1}$= 0.06, crosses - experimental data for KLT with 1% of Li at $T = 10$ K [3]. Intensity is represented in arbitrary units.

Figure 4. FOR scattering line shape, solid line - theory at $\alpha_2\Delta$ =0.55 and $(\tau\Delta)^{-1}$= 0.15, crosses - experimental data for KLT with 4% of Li at $T = 55$ K [3]. Intensity is represented in arbitrary units.

Figure 5. FOR scattering line shape of KTN with 15.7% of Nb at $T = 150$ K [2] (*b*); calculated line shape for $\alpha_2\Delta$ =0.21, $(\tau\Delta)^{-1}$= 0.004 (*a*).

Figure 6. FOR scattering line shape, solid line - theory at $\alpha_2\Delta$ =0.25 and $(\tau\Delta)^{-1}$= 0.0036, doted line - for KTN with 15.7% of Nb at $T = 142$ K [2].

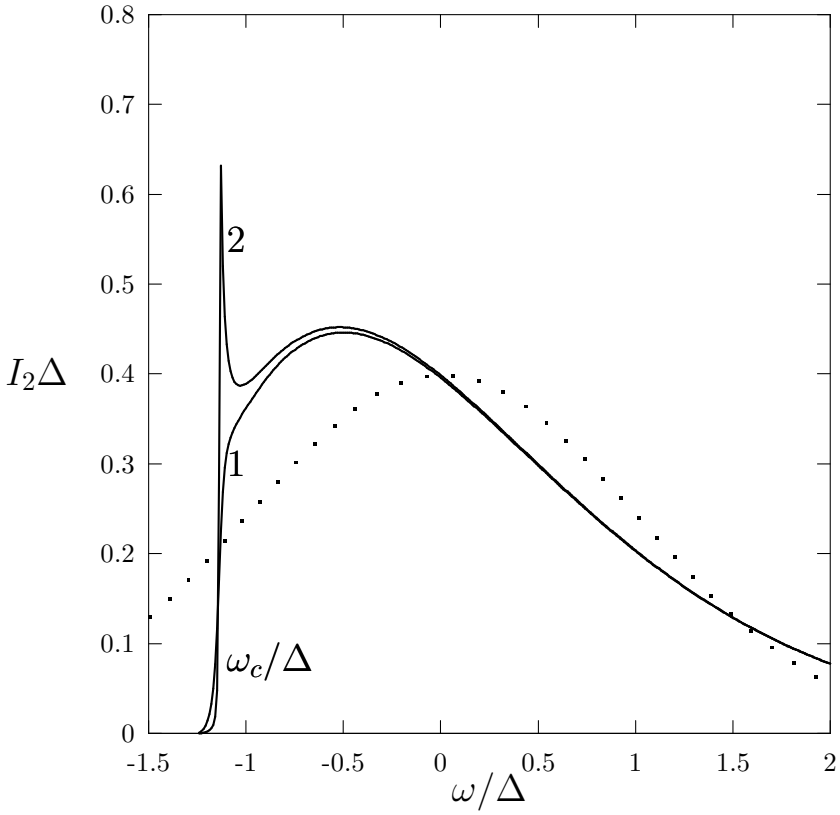
0.8
0.7
0.6
0.5
0.4
0.3
0.2
0.1
0
$I_2\Delta$
2
1
ω_c/Δ
-1.5
-1
-0.5
0
0.5
1
1.5
2
ω/Δ

Figure 1

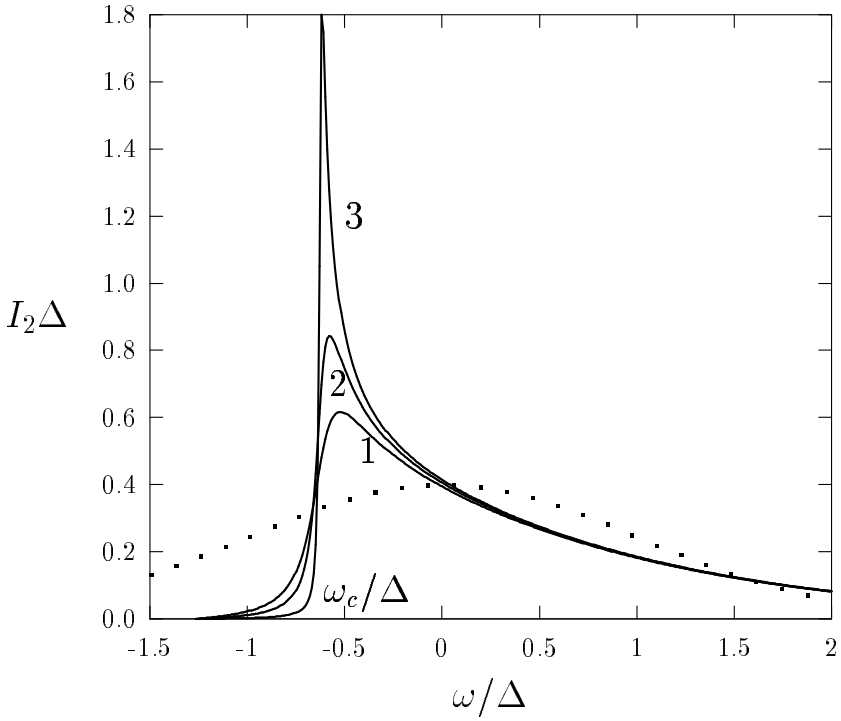
1.8
1.6
1.4
1.2
1.0
0.8
0.6
0.4
0.2
0.0
$I_2\Delta$
3
2
1
ω_c/Δ
-1.5
-1
-0.5
0
0.5
1
1.5
2
ω/Δ

Figure 2

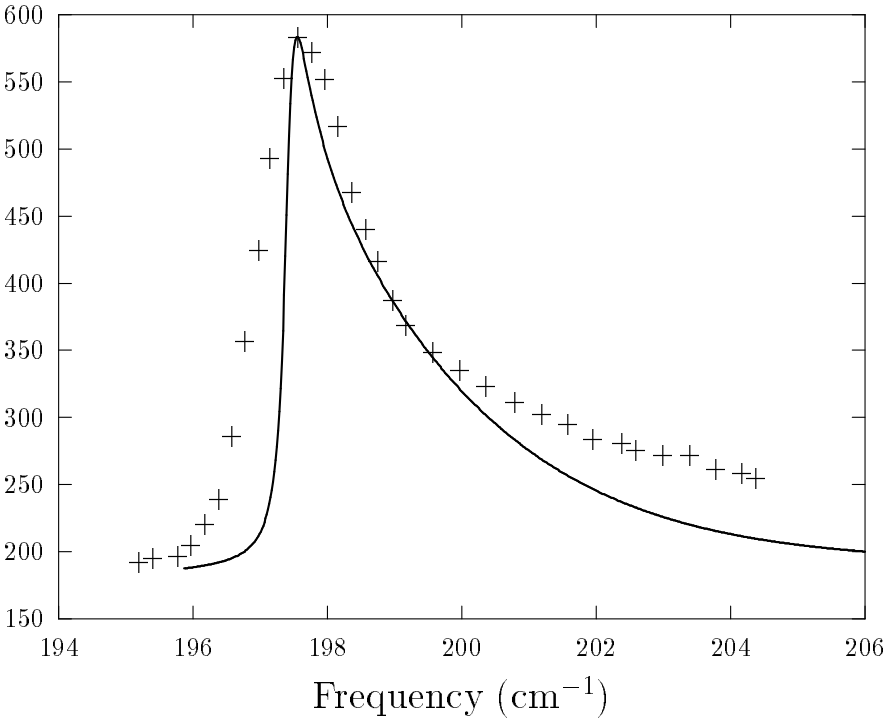
600
550
500
450
400
350
300
250
200
150
194
196
198
200
202
204
206
Frequency (cm^{-1})

Figure 3

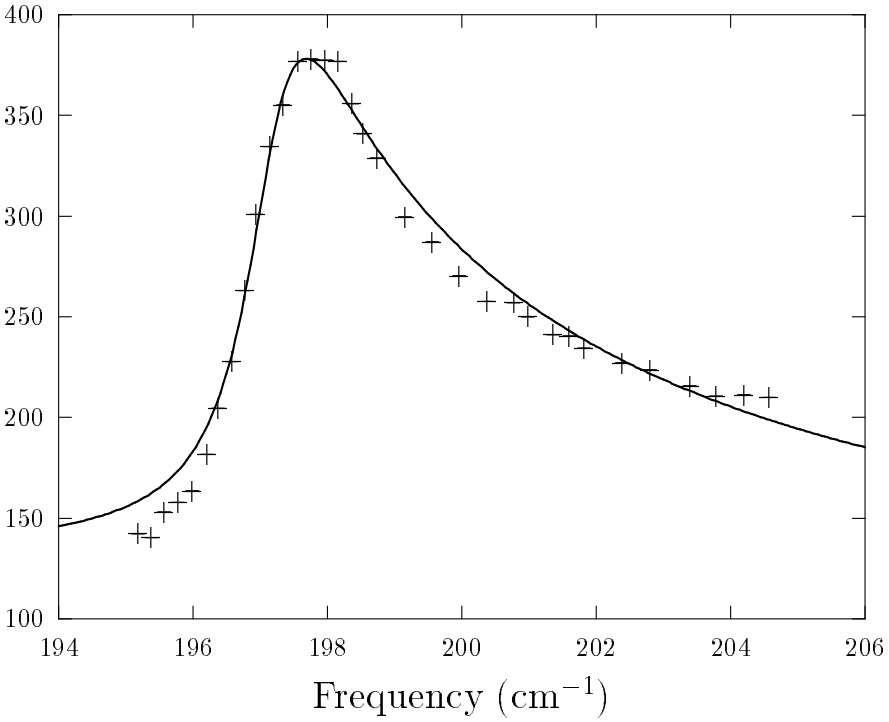
400
350
300
250
200
150
100
194
196
198
200
202
204
206
Frequency (cm^{-1})

Figure 4

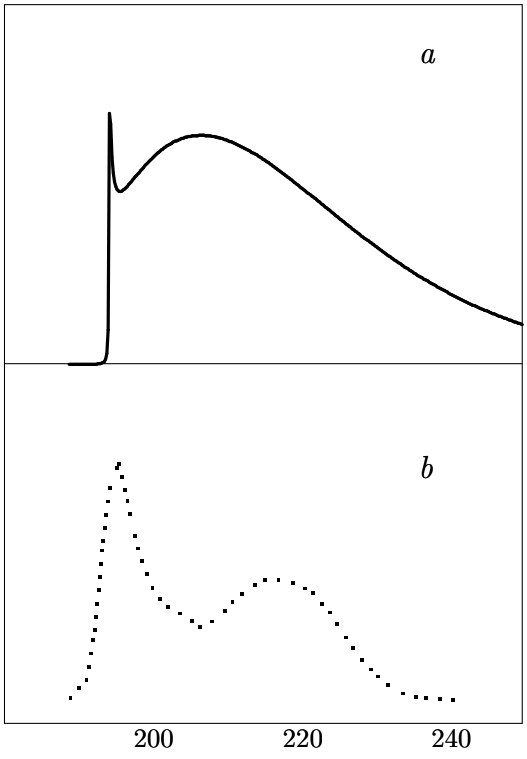

Figure 5

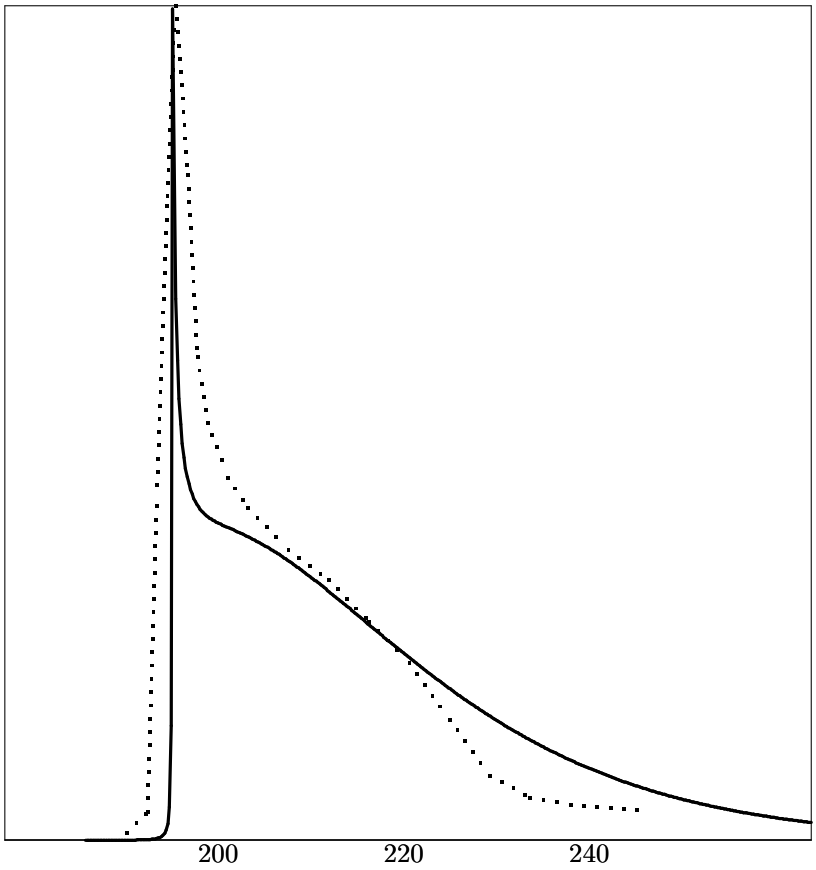

Figure 6